

Adsorption and catalytic oxidation of asphaltenes in fumed silica nanoparticles: Effect of the surface acidity

Camilo Andrés Franco-Ariza, Juan David Guzmán-Calle & Farid Bernardo Cortés-Correa

Facultad de Minas, Universidad Nacional de Colombia, Medellín, Colombia. caafancoar@unal.edu.co, jdguzmanc@unal.edu.co, fbcorres@unal.edu.co

Received: March 11th, 2016. Received in revised form: April 15th, 2016. Accepted: May 25th, 2016

Abstract

This study aims to evaluate the effect of surface acidity of fumed silica nanoparticles in adsorption and subsequent thermal cracking of Colombian asphaltenes. The acidities of the surfaces were established through Temperature Programmed Desorption (TPD) experiments. The adsorption equilibrium of asphaltenes was determined using a static batch method, and the data obtained was fitted using the Langmuir model, the Freundlich model and the SLE Model. Asphaltene catalytic oxidation experiments were conducted, and it was found that this process was surface nature dependent. In all cases, the temperature of asphaltene oxidation was reduced regarding the virgin asphaltene sample. The effective activation energies were estimated with the iso-conversional OFW method. This energy was found to be related to adsorption affinity and asphaltene self-association on nanoparticles surface.

Keywords: asphaltenes; adsorption isotherms; thermal cracking; nanoparticles; superficial modification.

Adsorción y oxidación catalítica de asfaltenos en nanopartículas de sílice fumárica: Efecto de la acidez superficial

Resumen

Este trabajo busca evaluar el efecto de la acidez superficial de nanopartículas de sílice fumárica en la adsorción y craqueo térmico de asfaltenos colombianos. La acidez de las superficies fue determinada a través de pruebas TPD. Los experimentos de adsorción fueron elaborados utilizando un método por lotes y los datos obtenidos fueron ajustados al modelo de Langmuir, al modelo de Freundlich y al modelo SLE. Se llevó a cabo la oxidación catalítica de los asfaltenos y se encontró que este proceso era dependiente de la superficie en que se llevaba a cabo. En todos los casos, la temperatura de oxidación de los asfaltenos fue reducida en consideración con los asfaltenos vírgenes. Las energías de activación fueron estimadas con el método isoconversional OFW. Se encontró que esta energía está relacionada con la afinidad del proceso adsorptivo y la auto-asociación de los asfaltenos en la superficie de la nanopartícula

Palabras clave: asfaltenos; isoterma de adsorción; craqueo térmico; nanopartículas; modificación superficial.

1. Introduction

According to a projection made by the Organization of the Petroleum Exporting Countries (OPEC), a growth in energetic global demand of at least 50% is expected over the next decades [1]. Demand will increase from 267.6 million barrels of oil equivalent per day (mboe/d) in 2013 to 399.4 mboe/d in 2040 [1]. In this year it is also expected that 53% of this demand will be supplied by hydrocarbon industry [1]. In this scenario, it is

worthwhile noting that Extra-Heavy Oil (EHO) reserves correspond to 32% of world oil reserves [2]; therefore, it is necessary to investigate about this kind of crude oil could as an alternative to supplying the energy demand. EHO have a lot of heavy hydrocarbon compounds such as asphaltene that reduce the American Petroleum Institute gravity ($^{\circ}$ API) and drastically increase oil viscosity [3,4]. Therefore, asphaltene are defined as the heaviest fraction of the crude oil soluble in aromatics hydrocarbons, but it is insoluble in alkanes such as n-pentane

How to cite: Franco-Ariza, C.A.; Guzmán-Calle, J.D.; & Cortés-Correa, F. B. Adsorption and catalytic oxidation of asphaltenes in fumed silica nanoparticles: effect of the surface acidity DYNA 83 (198) pp. 171-179, 2016.

and *n*-heptane [5, 6]. Generally, it has a polyaromatic core that is attached to alkyl chains and heteroatoms like O, N, S, Ni, V and Fe [7-10]. Some problems associated with these compounds are the reduction of oil mobility at reservoir conditions, changes in the reservoir wettability, and their deposition over refining equipment [11]. Typically, asphaltenes are removed by solvent injection, vapor injection, or mechanically [12-14], but these techniques, in most the cases, can lead to re-deposition and then a lower Energy Return On Investment (EROI) [15]. In summary, the presence of asphaltenes can affect production, transportation and the refinery processes, involving a large amount of capital and operational costs because conventional recovery techniques cannot be used effectively [16].

In this sense, new cost-effective and environmentally friendly technologies that enhance EHO from unconventional resources with lower operational and capital costs are a priority. As such, nanoparticles have recently become an area of research that is attractive for the oil industry [5, 16-26]. The adsorption and subsequent thermal decomposition of asphaltenes onto surfaces of nanoparticles was first introduced by Nassar and colleagues [5,16,17,26-31]. In his earlier study [5], he investigated the effect of different metal oxides in the adsorption process and post-oxidation, pyrolysis or gasification of asphaltenes. He found that these processes are adsorbent specific. Recently, at the Universidad Nacional de Colombia, several studies have been conducted on functionalized nanoparticles for asphaltenes adsorption and post-decomposition [19,20,23,25].

A in-depth and extensive investigation into different key variables, such as asphaltenes' chemical structure and nanoparticles functionalities will provide insight into the mechanism and behavior of nanoparticles' efficiency as catalysts and inhibitors. This will result in enhanced oil recovery techniques and quality improvements. For this reason, this paper is the continuation of our work, and its primary objective is to modify the fumed silica nanoparticles surface in order to obtain different acidities and then evaluate their effect on the adsorption and catalytic oxidation of asphaltenes. Also, a correlation between the calculated effective activation energies and the Langmuir model, the Freundlich model, and the SLE model parameters are presented to provide a better understanding of the role of the adsorption process in asphaltenes catalytic decomposition.

2. Materials and methods

2.1. Materials

A Colombian crude oil with 7.9°API, a viscosity of 595688 cP at 25°C, and approximately 13 wt% of asphaltenes content is used as the asphaltenes source. These were extracted by *n*-Heptane (99%, Sigma-Aldrich, St. Louis, MO). Toluene (99.5%, Merck GaG, Germany) was used to prepare heavy oil model solutions. Fumed silica nanoparticles, HCl (37%), and NH₄OH (28%) were used for superficial modifications and were purchased from Sigma-Aldrich (St. Louis, MO). To determine superficial acidity, 10% NH₃/He and He (99.9%) gasses were provided by Linde (Medellín, Colombia).

2.2. Methods

2.2.1. Asphaltenes extraction

Solid *n*-C₇ asphaltene was extracted from the crude oil by adding an excess amount of *n*-heptane following a standard procedure described in previous studies [5, 19]. 40 mL of *n*-heptane are added to the crude oil per every gram of it that was used. The mixture is sonicated for 2 h at 25°C and then stirred at 300 rpm for 20 h. Samples are further centrifuged at 5000 rpm for 15 min. The precipitated is filtered through 8 µm Whatman filter paper and washed with *n*-heptane until the color of the asphaltenes became shiny black. Finally, the asphaltenes obtained were homogenized and fined using a mortar and left to dry in a vacuum oven at room temperature (RT) for 12 h.

2.2.2. Nanoparticles surface modification

The nanoparticles' surface is modified to neutral, basic or acidic by adding the nanoparticles to aqueous solutions with different pH values of 3, 7 and 10. The pH is adjusted by adding aliquots of HCl or NaOH at 0.1N. The mixture is sonicated at (RT) for 2 hours. Then, the nanoparticles are separated and washed with deionized water until the pH value of the residue remains constant. Finally, the product is dried at 120°C for 6 hours to eliminate any humidity.

2.2.3. Particle size and surface area measurements

The sizes of the nanoparticles were obtained using an XPert PRO MPD X-ray diffractometer (PANalytical, Almelo, Netherlands) with Cu K α radiation operating at 60 kV and 40 mA with a $\theta/2\theta$ goniometer. The mean nanoparticle diameter (crystallite size) was determined by applying the Scherrer equation to the principal diffraction peak. Additionally, the surface areas (S_{BET}) were measured using a ChemBET 3000 (Quantachrome Instruments, Florida, USA) by employing the Brunauer-Emmet-Teller (BET) method [32,33]. This was undertaken by degassing the samples overnight at 140°C under a N₂ flow and after performing nitrogen adsorption-desorption at -196°C.

2.2.4. Temperature Programmed Desorption

NH₃ temperature programmed desorption (TPD) measurements were carried out with 0.1 g samples at a flow rate of 80 mL/min. Before the TPD measurements were made, nanomaterials were pretreated in a flow of Helium at 110°C for 3 h. Then, samples were treated with 10% NH₃/He at 100°C for 1 h ensuring NH₃ saturation and purged with He for 1 h. TPD runs were carried out between 100°C to 900°C at a heating rate of 10°C/min. The online ChemBet 3000 (Quantachrome Instruments, Florida, USA) with a Thermal Conductivity Detector (TCD) was used to monitor the desorbed NH₃.

2.2.5. Equilibrium adsorption isotherms

Model solutions for the batch adsorption experiments are prepared by dissolving a desired amount of the obtained

asphaltenes in toluene. All samples were made from a stock solution that was prepared at a maximum concentration (C_{max}) of 5000 mg/L without asphaltenes precipitation. The initial concentration of asphaltene solutions used in the adsorption experiments ranged from 500 mg/L to C_{max} . Before the experiments were undertaken, a calibration curve of absorbance against concentration was constructed at a wavelength of 295 nm [34], using a Genesys 10S UV-VIS spectrophotometer (Thermo Scientific, Waltham, MA). Nanoparticles are added to the solutions in a relation of 100mg/10 mL. The solutions are stirred at 300 rpm for 24 h at 25°C to ensure that they were in equilibrium. The amount adsorbed q in units of mg of asphaltenes / m² of nanoparticles surface area is estimated according to eq. (1):

$$q = \frac{C_0 - C_E}{A} V \quad (1)$$

where C_0 (mg/L) and C_E (mg/L) are the initial concentration of asphaltenes in the solution and the equilibrium concentrations of asphaltenes in the supernatant, respectively; V (L) the solution volume and A (m²) the nanoparticles' dry surface areas.

2.2.6. Thermogravimetric analysis

After the adsorption experiments, the nanoparticles with asphaltenes adsorbed are extracted from the solutions by centrifugation for 15 min at 4000 rpm using a Hermle Z 306 Universal Centrifuge (Labnet, NJ) and dried overnight in a vacuum oven. Thermogravimetric analysis is performed on a fixed amount of asphaltenes that adsorbed 0.2 mg/m² using a Q50 Thermogravimetric Analyzer (TGA) made by TA Instruments, Inc. (New Castle, DE). The TGA analyzer is coupled to an IRAffinity-1 FTIR device (Shimadzu, Japan) that is equipped with a gas cell to analyze the outcome gasses. The samples (nanoparticles with asphaltene adsorbed and virgin nanoparticles) are heated in an air atmosphere from 30 to 1000°C at the following different heating rates: 5, 10, and 20°C/min. The air-flow was kept at a constant 100 mL/min during the experiment. It is worthwhile mentioning that the sample mass was kept low at approximately 5 mg to avoid any diffusion limitations [19, 35, 36].

2.3. Modeling

The experimental data obtained for adsorption isotherms were modeled using two commonly used adsorption models: the Langmuir model and the Freundlich model [37, 38]. Likewise, the experimental results were modeled using a novel Solid-Liquid Equilibrium model [39]. For the kinetic oxidation of the asphaltenes on nanoparticles, the Ozawa-Flyn-Wall (OFW) method was applied. This allows the reaction kinetics to be described and the effective activation energy to be estimated [40].

2.3.1. The Langmuir model

The Langmuir model has been widely used since it was published in 1916 to correlate experimental data on equilibrium adsorption [37]. In order to do this, monolayer

adsorption takes place on a homogeneous surface and it was derived by taking into account the fact that equilibrium is obtained when the rates of adsorption and desorption are equivalent. The Langmuir equation can be expressed as follows:

$$N_{ads} = N_{ads,max} \left(\frac{K_L C_E}{1 + K_L C_E} \right) \quad (2)$$

where $N_{ads,max}$ (mg/m²) is the amount of asphaltenes adsorbed onto the nanoparticles, C_E (mg/L) is the equilibrium concentration of asphaltenes in the supernatant, K_L (L/mg) is the Langmuir equilibrium adsorption constant related to the affinity of binding sites, and $N_{ads,max}$ (mg/m²) is defined as the monolayer saturation capacity. The latter represents the maximum amount of asphaltenes adsorbed per unit of nanoparticle surface area for complete monolayer coverage.

2.3.2. The Freundlich model

The Freundlich approach was created in 1906. It is an empirical expression that represents the isothermal variation of the adsorption of a quantity of mass, which is adsorbed by unit of surface area (of solid adsorbent) at equilibrium concentration [38]:

$$N_{ads} = K_F C_E^{1/n} \quad (3)$$

where K_F ((mg/m²)/(L/mg)^{1/n}) is the Freundlich constant related to the adsorption capacity, and $1/n$ (unitless) is the adsorption intensity factor.

2.3.3. The Solid-Liquid Equilibrium (SLE) model

Recently, Montoya et al. [39] proposed a three-parameter model to describe the adsorption isotherms of asphaltene by non-porous materials. The model is based on a theoretical framework of adsorption by self-associated asphaltenes on solid surfaces. The SLE model equation is expressed as follows:

$$C_E = \frac{\psi H}{1 + K\psi} \exp\left(\frac{\psi}{q_m A}\right) \quad (4)$$

with

$$\psi = \frac{-1 + \sqrt{1 + 4K\xi}}{2K} \quad (5)$$

and

$$\xi = \left(\frac{q_m q}{q_m - q}\right) A \quad (6)$$

where q (mg/m²) is the amount of asphaltenes adsorbed by the nanoparticle surface, q_m (mg/m²) is the maximum adsorption capacity of the nanoparticles, A (m²/mg) is the measured surface area per mass of nanoparticles and C_E (mg/g) is the equilibrium concentration of asphaltenes in the supernatant. K (g/g) is the reaction constant related to the asphaltenes' degree of association on the nanoparticles surface, and H (mg/g) is the Henry's law constant linked to the asphaltenes' preference for being in the liquid phase or

the adsorbed phase [39]. The H , K and q_m SLE parameters were estimated by model fitting.

For the three adsorption models, the correlation coefficient (R^2) and a nonlinear chi-square (χ^2) analysis were used to estimate the goodness of fit using the Solver feature that is part of the Excel package [41].

2.3.4. OFW model

After TGA experiments were performed at different heating rates, the OFW method can be used to estimate the effective activation energies [40,42]. The Ozawa-Flynn-Wall method (OFW) gave us an estimate of the effective activation energies, assuming that for a constant reaction conversion, the reaction rate, eq. (7), is a function of the temperature and the state.

$$\frac{d\alpha}{dt} = K_\alpha \exp\left(-\frac{E_\alpha}{RT}\right) f(\alpha) \quad (7)$$

where K_α (1/s) is the pre-exponential factor, E_α (kJ/mol) is the effective activation energy for a constant conversion, R (J/mol·K) is the ideal gas constant, T (K) is the reaction temperature and α is the reaction conversion described by the next equation:

$$\alpha = \frac{m_0 - m_T}{m_0 - m_f} \quad (8)$$

with m_0 as the initial mass of the sample; m_f the final mass of the sample and m_T the mass at a given temperature. Eq. (9) can be obtained when the heating rate is defined as $\beta = dT/dt$ and integrating. Using the Doyle approximation [43], the effective activation energy can be estimated from the slope of the linear fit from the plot of $\log(\beta)$ against $1/T$, according to eq. (10)[35]:

$$g(\alpha) = \int_0^\alpha \frac{d\alpha}{f(\alpha)} = \int_0^T \frac{K_\alpha \exp(-E_\alpha/RT)}{\beta} dT \quad (9)$$

$$\log(\beta) = \log\left(\frac{K_\alpha E_\alpha}{Rg(\alpha)}\right) - 2,315 - 0,4567 \frac{E_\alpha}{RT} \quad (10)$$

3. Results and discussion

3.1. Characterization of nanoparticles

Silica nanoparticles are usually synthesized through Sol-Gel method [44,45]. As mentioned above, commercial silica nanoparticles were used. After the superficial modification process that was described above, the acidic silica nanoparticles (AS), the neutral (NS) and basic silica nanoparticles (BS) show the same particle diameter (d_p); this can be seen in Table 1. It can be seen that the superficial modification apparently has no effect on the size of the nanoparticle. On the other hand, the surface area (S_{BET}) decreased when the particle became more acidic. This was determined with total acidity that is related to the amount of NH_3 adsorbed by each nanoparticle. In this case, it can be noticed that superficial treatments were effective because AS is the most acidic of three materials.

Table 1.
Nanoparticles characterization.

Nanoparticle	d_{p-50} (nm)	S_{BET} (m ² /g)	Total acidity (μmol/g)
AS	7	237.9	2847
NS	7	171.8	2156
BS	7	138.1	1285

Source: The authors

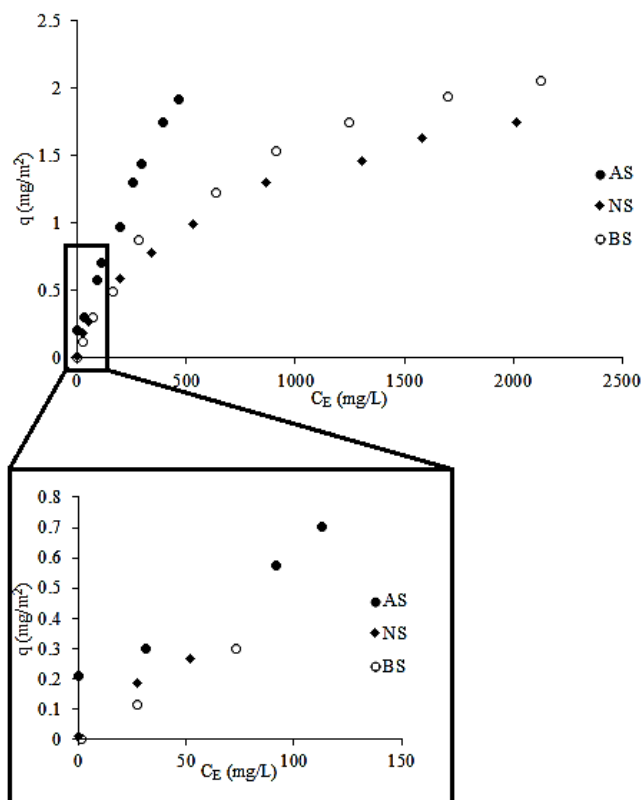


Figure 1. a) Adsorption isotherms of asphaltenes by fumed silica nanoparticles with different surface acidities at 25°C and b) zoom on Henry's region.

Source: The authors

3.2. Asphaltenes adsorption isotherms

Fig. 1a shows the obtained adsorption isotherms of asphaltenes by AS, NS and BS that were constructed at 25°C on surface area basis. It can be observed that the trend of the amount adsorbed at C_E of 464 mg/L, where the isotherms can be compared, follows the order $AS > BS > NS$, which indicates that the surface is selective to determined functional groups that are present in the asphaltenes structure.

Also, Fig. 1b shows that in the Henry's region, the adsorption affinity is also surface specific. As the Langmuir model K_L is related to the affinity of binding sites, larger values implied more adsorption affinity [17,19,20]. In the empirical model proposed by Freundlich, this affinity cannot be seen so clearly. Hence, frequently K_F is taken as a rough indicator of the adsorption capacity and $1/n$ is the adsorption intensity factor. A larger K_F value suggests greater adsorption capacity, and a lower $1/n$ indicates stronger adsorption strength [17,19]. Furthermore, the reciprocal of the parameter

Table 2.

Langmuir, Freundlich and SLE model parameters of asphaltenes adsorption by AS, NS and BS at 25°C.

	Parameter	AS	NS	BS
Langmuir model	$N_{ads,max}$ (mg/m ²)	4.43	2.22	2.71
	K_L (L/mg) x 10 ⁻³	1,602	1,580	1,409
	R^2	0.986	0.991	0.998
	χ^2	9.858	0.209	0.027
Freundlich model	K_F ((mg/m ²)/(L/mg) ^{1/n})	0.025	0.047	0.043
	1/n (unitless)	0.71	0.48	0.51
	R^2	0.989	0.996	0.988
	χ^2	2.156	0.018	0.113
SLE model	H (mg/g)	0.15	0.25	0.28
	K (g/g) x 10 ⁻⁴	2.45	1.75	1.45
	q_m (mg/m ²)	7.75	3.49	4.58
	R^2	0.99	0.99	0.99
	χ^2	1.30	1.43	0.58

Source: The authors

H in the SLE model is a clear indicator of the adsorption affinity. A smaller H value implies greater adsorption affinity [21,39]. In this regard, we can see in Table 2 that the adjusted parameters for the Langmuir and SLE models indicate higher adsorption affinity with the most acidic nature of the surface of the nanoparticle. Also, the SLE model tells us that the trend followed by the K parameter is opposite to the one observed for the H parameter, meaning that BS nanoparticles lead to a lower degree of asphaltenes self-association over its surface. Freundlich model's parameters do not show a direct relationship with the acidic nature of the surface.

3.3. Catalytic Oxidation of Asphaltenes

The TGA experiments for asphaltenes oxidation were conducted at three different heating rates: 5, 10 and 20°C/min with an oxygen flow at 100 cm³/min. Fig. 2a-d shows the conversion for oxidation of a) virgin asphaltenes and asphaltenes in the presence of b) AS, c) NS and d) BS. For all systems, it can be observed that the percentage of conversion decreases as the heating rate increases.

To show a comparison, Fig. 3 shows the conversion of asphaltenes in the presence and absence of the evaluated nanoparticles at a fixed heating rate of 10°C/min. It is observed that for a fixed value of conversion, the temperature increases in the order of BS < NS < AS < virgin asphaltenes. This confirms the catalytic effect of the nanoparticles and shows that catalytic oxidation of the asphaltenes is specific to the adsorbent surface conditions. It can also be noted that the catalytic effect of the surface is related to the adsorption affinity and asphaltenes self-association. As lower signifies adsorption affinity (higher value of H at SLE model) and as lower signifies asphaltenes self-association (lower value of K at SLE model), higher is the catalytic behavior of the surface.

Fig. 4 shows the rate of mass loss for virgin asphaltenes oxidation and asphaltenes oxidation in the presence of AS, NS and BS. It can be seen in Fig. 4 that asphaltenes oxidation starts before for those asphaltenes adsorbed onto the nanoparticles, in comparison with the virgin asphaltenes. It is worthwhile mentioning that the virgin nanoparticles were also submitted for TGA analysis. For the virgin asphaltenes,

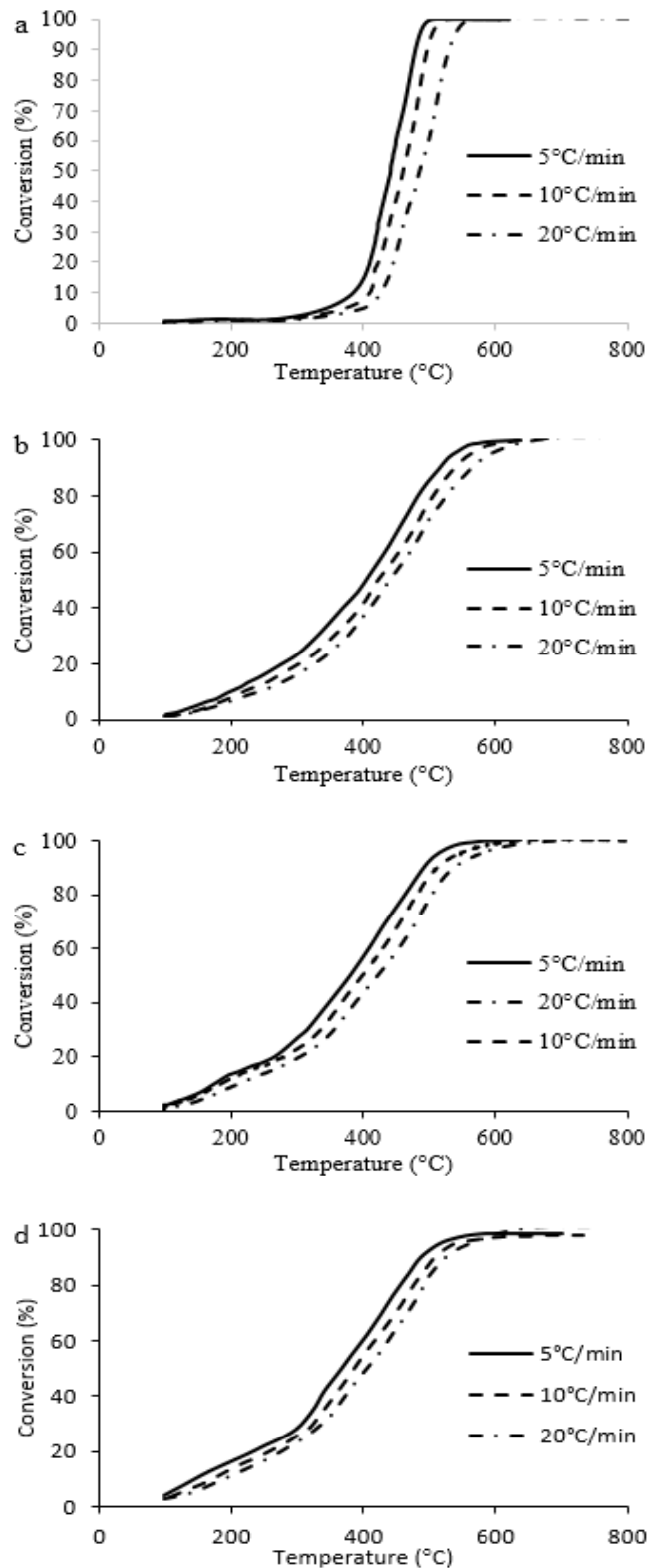


Figure 2. Conversion of a) virgin asphaltenes and asphaltenes in the presence of b) AS, c) NS and d) BS at different heating rates.

Source: The authors

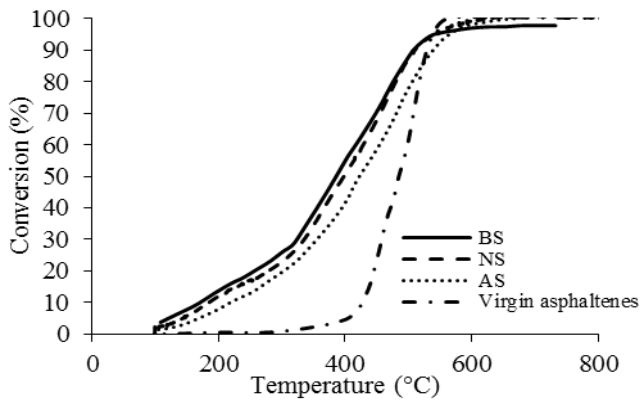


Figure 3. Conversion for oxidation of asphaltenes in the presence and absence of AS, NS and BS nanoparticles at a heating rate of 10°C/min. Source: The authors

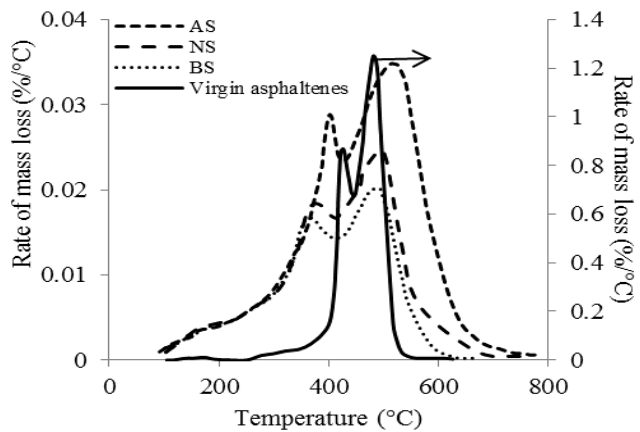


Figure 4. Rate of mass loss for oxidation of asphaltenes in presence and absence of AS, NS and BS nanoparticles at a heating rate of 10°C/min. Source: The authors

two peaks are observed at approximately 422 and 479 °C. The first peak temperature is considerably reduced by the nanoparticles at 38, 52 and 67°C. This indicates that the catalytic activity of the BS is higher than that of the other two nanoparticles. These results agree with the estimated values of the *H* and *K* parameters of the SLE model.

The evolution of gas production was also evaluated using an FTIR device coupled with the TGA analyzer. Figs. 5a-d show the evolution of CO, CO₂, CH₄ and other light hydrocarbon production to oxidize a) virgin asphaltenes and asphaltenes in the presence of b) AS, c) NS and d) BS at a fixed heating rate of 10°C/min. It is worthwhile mentioning that the results are normalized based on the signal with the highest intensity that corresponds to the CO₂ production. In all cases, it is observed that the major production corresponds to the CO₂. Except for the system with BS, the trend of effluent production increases in the order of CO < CH₄ < Hydrocarbons < CO₂. However, for the BS, the trend followed is CH₄ < Hydrocarbons < CO < CO₂.

3.4. Estimation of activation energies

The results for the effective activation energies (EAE) are shown in Fig. 6. The asphaltenes follow an increasing trend

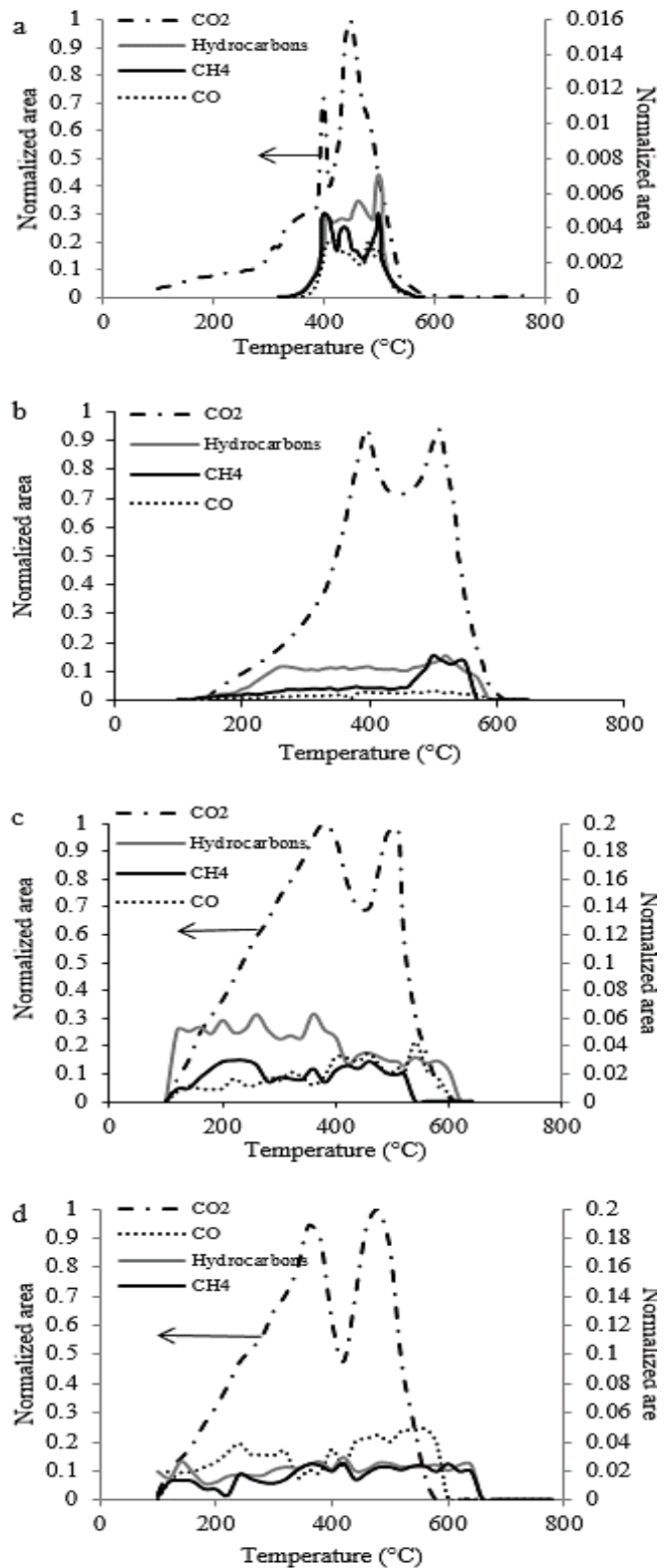


Figure 5. Evolution of CO, CO₂, CH₄ and other hydrocarbon production for oxidation of a) virgin asphaltenes and asphaltenes in the presence of b) AS, c) NS and d) BS at a heating rate of 10°C/min. Source: The authors

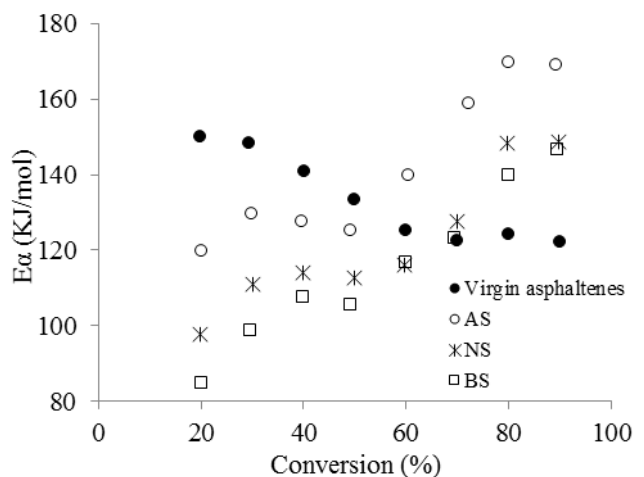


Figure 6. Estimated effective activation energies for asphaltenes oxidation in the presence and absence of AS, NS and BS nanoparticles. Source: The authors

in the presence of the nanoparticles, which increase as the asphaltenes conversion increases. This could be due to addition reactions that occur in the process. However, for the virgin asphaltenes, the trend observed is the opposite. Both behaviors are indicative of the fact that asphaltene oxidation in the presence and absence of the nanoparticles is not a single-step process and it involves more than one mechanism. Fig. 6 shows that higher EAE are obtained for AS, followed by NS, and the lower values are obtained for BS. Also, the pathway followed by the EAE is similar for the three nanoparticles, indicating that the reaction order is possibly similar for the three catalysts.

Fig. 7 shows the correlation of parameters H and K from the SLE model and K_L from the Langmuir model. These have the estimated EAE for the following percentages of conversion: 20, 50 and 80%. It can be observed that as the adsorption affinity increases (i.e. the H parameter decreases in the SLE model and the K_L parameter increases in the Langmuir model), the EAE increases. This indicates that an over attachment of the asphaltenes in the catalysts surface would lead to a decrease in the catalytic activity of the nanoparticles. However, the correlation observed for the K parameter indicates that as the degree of asphaltenes self-association increases the catalytic activity of the nanoparticles decreases. This is also shown in Fig. 8 where the evolution of CO is correlated with the K parameter for different degrees of conversion. It is observed that as the degree of asphaltenes self-association decreases, the production of CO increases. This could be due to bigger asphaltenes aggregates tending to hide some active sites that are released as asphaltenes are oxidized. This leads the CO to be chemisorbed over the nanoparticle surfaces to form CO₂.

4. Conclusions

The surface modification process effectively modified the acidity of nanoparticle surfaces, as can be seen in TPD experiments. Through batch adsorption experiments, the isotherms of asphaltenes adsorption onto fumed silica with different surface acidities were successfully constructed. The

Langmuir model, the Freundlich model, and the SLE model have an excellent adjustment for the experimental results of the adsorption isotherms. The first and the third of these models, allow us to conclude that the acidic surface creates a greater affinity for the asphaltenes in the adsorption process, but it leads to higher EAE and to disfavor catalytic activity. Also, if the asphaltenes self-association is higher on the nanoparticle surface, represented in parameter K of the SLE model, the catalytic activity is lower. In this sense, the BS showed a better performance in the catalytic oxidation of asphaltenes. Also, it was possible to detect the effluent gasses in the oxidation process by using a coupled FTIR device, which showed that they are surface nature dependent.

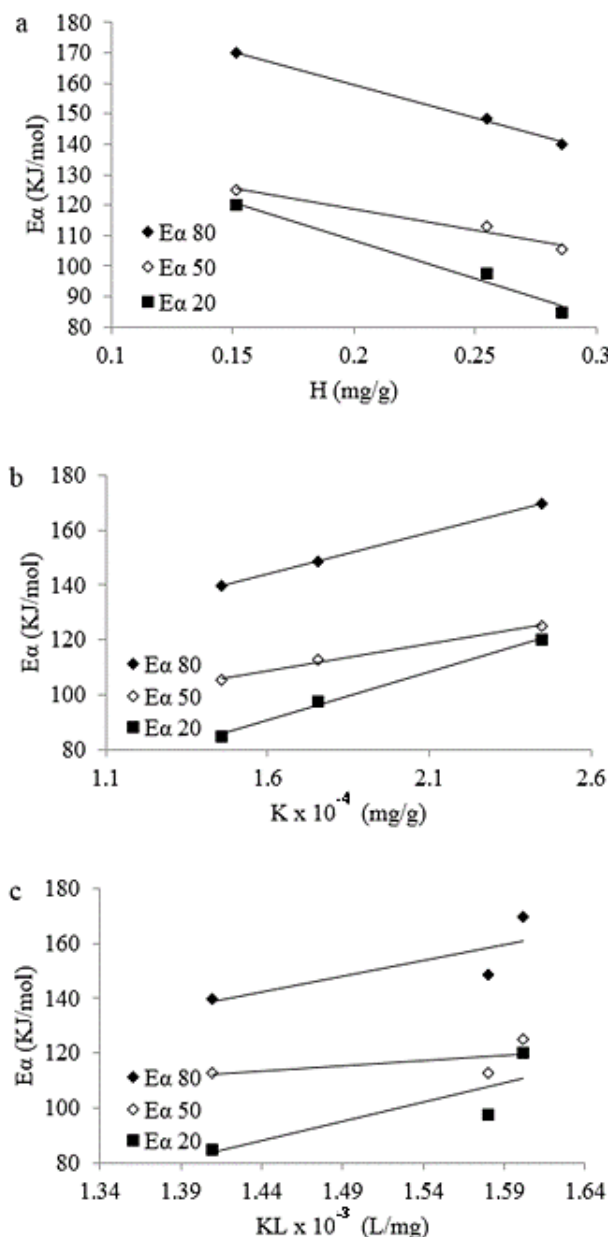


Figure 7. Correlation of the a) H and b) K SLE parameters and c) K_L Langmuir parameter, with the estimated effective activation energies for percentages of conversion of 20, 50 and 80%. Source: The authors

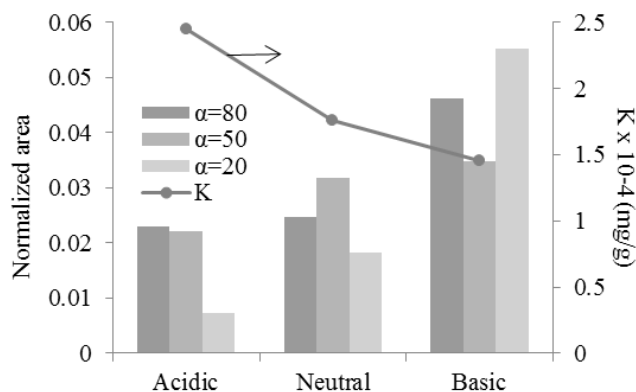


Figure 8. Correlation of the CO production and the K parameter of the SLE model at percentages of conversion of 20, 50 and 80%.

Source: The authors

References

- [1] OPEC, 2015 World Oil Outlook, Vienna, Austria, OPEC Secretariat, 2015, pp. 29-88.
- [2] IEA, World Energy Outlook 2012, Paris, France, International Energy Agency, 2012, pp. 81-120.
- [3] Ghanavati, M., Shojaei, M.-J. and Ramazani, A., Effects of asphaltene content and temperature on viscosity of Iranian heavy crude oil: experimental and modeling study. *Energy & Fuels*, 27(12), pp. 7217-7232, 2013. DOI: 10.1021/ef400776h.
- [4] Leontaritis, K., Amaefule, J. and Charles, R., A systematic approach for the prevention and treatment of formation damage caused by asphaltene deposition. *SPE Production & Facilities*, 9(03), pp. 157-164, 1994. DOI: 10.2118/23810-PA.
- [5] Nassar, N.N., Asphaltene adsorption onto alumina nanoparticles: kinetics and thermodynamic studies. *Energy & Fuels*, 24(8), pp. 4116-4122, 2010. DOI: 10.1021/ef100458g.
- [6] Fergoug, T. and Bouhadda, Y., Determination of Hassi Messaoud asphaltene aromatic structure from ¹H & ¹³C NMR analysis. *Fuel*, 115, pp. 521-526, 2014. DOI: 10.1016/j.fuel.2013.07.055.
- [7] Acevedo, S., Castro, A., Negrin, J.G., Fernández, A., Escobar, G., Piscitelli, V., Delolme, F. and Dessalces, G., Relations between asphaltene structures and their physical and chemical properties: The rosary-type structure. *Energy & Fuels*, 21(4), pp. 2165-2175, 2007. DOI: 10.1021/ef070089v.
- [8] Groenzin, H. and Mullins, O.C., Asphaltene molecular size and structure. *The Journal of Physical Chemistry A*, 103(50), pp. 11237-11245, 1999. DOI: 10.1021/jp992609w.
- [9] Mullins, O.C., The asphaltenes. *Annual Review of Analytical Chemistry*, 4, pp. 393-418, 2011. DOI: 10.1146/annurev-anchem-061010-113849.
- [10] Mullins, O.C., Sabbah, H., Eyssautier, J.L., Pomerantz, A.E., Barré, L., Andrews, A.B., Ruiz-Morales, Y., Mostowfi, F., McFarlane, R. and Goual, L., Advances in asphaltene science and the Yen–Mullins model. *Energy & Fuels*, 26(7), pp. 3986-4003, 2012. DOI: 10.1021/ef300185p.
- [11] Adams, J.J., Asphaltene adsorption, a literature review. *Energy & Fuels*, 28(5), pp. 2831-2856, 2014. DOI: 10.1021/ef500282p.
- [12] Cenegy, L.M., Survey of successful world-wide asphaltene inhibitor treatments in oil production fields. in *SPE Annual Technical Conference and Exhibition (2001, New Orleans, Louisiana)*. Society of Petroleum Engineers, New Orleans, Louisiana, 2001, P. 7. DOI: 10.2118/71542-MS.
- [13] Allenson, S.J. and Walsh, M.A., A novel way to treat asphaltene deposition problems found in oil production. in *SPE international symposium on oilfield chemistry (1997, Houston, Texas)*. Society of Petroleum Engineers, Houston, Texas, 1997, pp. 699-702. DOI: 10.2118/37286-MS.
- [14] Torres, C.A., Treint, F., Alonso, C.I., Milne, A. and Lecomte, A., Asphaltene pipeline cleanout: A horizontal challenge for coiled tubing. in *SPE/ICoTA coiled tubing conference and exhibition (2005, The Woodlands, Texas)*. Society of Petroleum Engineers, The Woodlands, Texas, 2005, P. 19. DOI: 10.2118/93272-MS.
- [15] Zabala, R., Acuna, H.M., Cortes, F., Patino, J.E., Cespedes-Chavarro, C., Mora, E., Botero, O.F. and Guarin, L., Application and evaluation of a nanofluid containing nanoparticles for asphaltene inhibition in well CPSXL4. in *OTC Brasil (2013, Rio de Janeiro, Brazil)*. Offshore Technology Conference, Rio de Janeiro, Brazil, 2013, P. 14. DOI: 10.4043/24310-MS.
- [16] Nassar, N.N., Hassan, A. and Pereira-Almao, P., Application of nanotechnology for heavy oil upgrading: catalytic steam gasification/cracking of asphaltene. *Energy & Fuels*, 25(4), pp. 1566-1570, 2011. DOI: 10.1021/ef2001772.
- [17] Nassar, N.N., Hassan, A. and Pereira-Almao, P., Effect of surface acidity and basicity of aluminas on asphaltene adsorption and oxidation. *Journal of colloid and interface science*, 360 (1), pp 233-238, 2011. DOI: 10.1016/j.jcis.2011.04.056.
- [18] Franco, C.A., Nassar, N.N. and Cortés, F.B., Removal of oil from oil-in-saltwater emulsions by adsorption onto nano-alumina functionalized with petroleum vacuum residue. *Journal of colloid and interface science*, 433, pp. 58-67, 2014. DOI: 10.1016/j.jcis.2014.07.011.
- [19] Franco, C.A., Montoya, T., Nassar, N.N., Pereira-Almao, P. and Cortés, F.B., Adsorption and subsequent oxidation of colombian asphaltene onto nickel and/or palladium oxide supported on fumed silica nanoparticles. *Energy & Fuels*, 27(12), pp. 7336-7347, 2013. DOI: 10.1021/ef4018543.
- [20] Franco, C.A., Nassar, N.N., Ruiz, M.A., Pereira-Almao, P. and Cortés, F.B., Nanoparticles for inhibition of asphaltene damage: adsorption study and displacement test on porous media. *Energy & Fuels*, 27(6), pp. 2899-2907, 2013. DOI: 10.1021/ef4000825.
- [21] Franco, C.A., Nassar, N.N., Montoya, T., Ruiz, M.A. and Cortés, F.B., Influence of asphaltene aggregation on the adsorption and catalytic behavior of nanoparticles. *Energy & Fuels*, 29(3), pp. 1610-1621, 2015. DOI: 10.1021/ef502786e.
- [22] Hamed-Shokrlu, Y. and Babadagli, T., In-situ upgrading of heavy oil/bitumen during steam injection by use of metal nanoparticles: A study on in-situ catalysis and catalyst transportation. *SPE Reservoir Evaluation & Engineering*, 16(03), pp. 333-344, 2013. DOI: 10.2118/146661-PA.
- [23] Cortés, F.B., Mejía, J.M., Ruiz, M.A., Benjumea, P. and Riffel, D.B., Sorption of asphaltene onto nanoparticles of nickel oxide supported on nanoparticulated silica gel. *Energy & Fuels*, 26(3), pp. 1725-1730, 2012. DOI: 10.1021/ef201658c.
- [24] Hashemi, R., Nassar, N.N. and Pereira-Almao, P., Transport behavior of multimetallic ultradispersed nanoparticles in an oil-sands-packed bed column at a high temperature and pressure. *Energy & Fuels*, 26(3), pp. 1645-1655, 2012. DOI: 10.1021/ef201939f.
- [25] Nassar, N.N., Hassan, A. and Vitale, G., Comparing kinetics and mechanism of adsorption and thermo-oxidative decomposition of Athabasca asphaltene onto TiO₂, ZrO₂, and CeO₂ nanoparticles. *Applied Catalysis A: General*, 484, pp. 161-171, 2014. DOI: 10.1016/j.apcata.2014.07.017.
- [26] Nassar, N.N., Hassan, A. and Pereira-Almao, P., Effect of the particle size on asphaltene adsorption and catalytic oxidation onto alumina particles. *Energy & Fuels*, 25(9), pp. 3961-3965, 2011. DOI: 10.1021/ef2008387.
- [27] Nassar, N.N., Hassan, A. and Pereira-Almao, P., Clarifying the catalytic role of NiO nanoparticles in the oxidation of asphaltene. *Applied Catalysis A: General*, 462(463), pp. 116-120, 2013. DOI: 10.1016/j.apcata.2013.04.033.
- [28] Hassan, A., Lopez-Linares, F., Nassar, N.N., Carbognani-Arambarri, L. and Pereira-Almao, P., Development of a support for a NiO catalyst for selective adsorption and post-adsorption catalytic steam gasification of thermally converted asphaltene. *Catalysis Today*, 207(0), pp. 112-118, 2013. DOI: 10.1016/j.cattod.2012.05.010.
- [29] Nassar, N.N., Hassan, A., Carbognani, L., Lopez-Linares, F. and Pereira-Almao, P., Iron oxide nanoparticles for rapid adsorption and enhanced catalytic oxidation of thermally cracked asphaltene. *Fuel*, 95, pp. 257-262, 2012. DOI: 10.1016/j.fuel.2011.09.022.
- [30] Nassar, N.N., Hassan, A. and Pereira-Almao, P., Comparative oxidation of adsorbed asphaltene onto transition metal oxide

- nanoparticles. *Colloids and Surfaces A: Physicochemical and Engineering Aspects*, 384(1-3), pp. 145-149, 2011. DOI: 10.1016/j.colsurfa.2011.03.049.
- [31] Nassar, N.N., Hassan, A. and Pereira-Almao, P., Metal oxide nanoparticles for asphaltene adsorption and oxidation. *Energy & Fuels*, 25(3), pp. 1017-1023, 2011. DOI: 10.1021/ef101230g.
- [32] Brunauer, S., Emmett, P.H. and Teller, E., Adsorption of gases in multimolecular layers. *Journal of the American Chemical Society*, 60(2), pp. 309-319, 1938.
- [33] Rouquerol, F., Rouquerol, J. and Sing, K.S.W., *Adsorption by powders and porous solids; principles, Methodology and Applications*, London, U.K., Academic Press, 1999.
- [34] Goncalves, S., Castillo, J., Fernandez, A. and Hung, J., Absorbance and fluorescence spectroscopy on the aggregation behavior of asphaltene-toluene solutions. *Fuel*, 83(13), pp. 1823-1828, 2004.
- [35] Nassar, N.N., Hassan, A., Luna, G. and Pereira-Almao, P., Comparative study on thermal cracking of Athabasca bitumen. *Journal of thermal analysis and calorimetry*, 114(2), pp. 465-472, 2013.
- [36] Mateus, F.A.D., Chaves, A., Maradei, M.P., Fuentes, D.A., Guzman, A. and Picon, H.J., Kinetic analysis of the thermal decomposition of colombian vacuum residua by termogravimetry. *Ingeniería e Investigación*, 35(3), pp. 19, 2015. DOI: 10.15446/ing.investig.v35n3.49498.
- [37] Langmuir, I., The constitution and fundamental properties of solids and liquids. Part I. Solids. *Journal of the American Chemical Society*, 38(11), pp. 2221-2295, 1916.
- [38] Freundlich, H., Over the adsorption in solution. *J. Phys. Chem*, 57(385), pp. 385-470, 1906.
- [39] Montoya, T., Coral, D., Franco, C.A., Nassar, N.N. and Cortés, F.B., A novel solid-liquid equilibrium model for describing the adsorption of associating asphaltene molecules onto solid surfaces based on the "Chemical Theory". *Energy & Fuels*, 28(8), pp. 4963-4975, 2014.
- [40] Ozawa, T., A new method of analyzing thermogravimetric data. *Bulletin of the chemical society of Japan*, 38(11), pp. 1881-1886, 1965.
- [41] Montgomery, D.C. and Runger, G.C., *Applied statistics and probability for engineers*, John Wiley & Sons, 2010.
- [42] Flynn, J.H. and Wall, L.A., A quick, direct method for the determination of activation energy from thermogravimetric data. *Journal of Polymer Science Part B: Polymer Letters*, 4(5), pp. 323-328, 1966.
- [43] Doyle, C., Synthesis and evaluation of thermally stable polymers. II. Polymer evaluation. *Appl Polym Sci*, 5, pp. 285-292, 1961.
- [44] Fajardo, C.A.G. y Castellanos, F.J.S., Síntesis de catalizadores de Fe-Mo soportados sobre sílice para la oxidación selectiva de metano hasta formaldehído. *Ingeniería e Investigación*, 29(1), pp. 53-59, 2009.
- [45] Stöber, W., Fink, A. and Bohn, E., Controlled growth of monodisperse silica spheres in the micron size range. *Journal of colloid and interface science*, 26(1), pp. 62-69, 1968. DOI: 10.1016/0021-9797(68)90272-5.

C.A. Franco-Ariza, is a BSc. in Petroleum Engineer in 2012 and obtained a PhD degree in Energy Systems in 2015, both from the Universidad Nacional de Colombia, Medellín, Colombia. He has since dedicated his professional and research activities to nanotechnology applied to the oil & gas industry in different areas such as formation damage, heavy oil upgrading, EOR/IOR processes and wastewater remediation. Currently he is a researcher in the Chemistry and Petroleum Engineering Department, Facultad de Minas, Universidad Nacional de Colombia. Dr. Franco is the author of more than 20 published articles and presentations, and more than 10 International Conferences and Seminars.
ORCID: 0000-0002-6886-8338

J.D. Guzmán-Calle, is a BSc. an Economist in 2012 and as Petroleum Engineer in 2015 from Universidad de Antioquia and Universidad Nacional de Colombia, respectively, both in Medellín, Colombia. For the past three years he has been dedicated to research activities relating to development and application of nanotechnology in the oil and gas industry, specifically in different areas such as formation damage, heavy oil upgrading, fracking

fluids, EOR/IOR processes and wastewater remediation. Currently he is pursuing a MSc degree in Petroleum Engineering, Facultad de Minas, Universidad Nacional de Colombia.
ORCID: 0000-0002-3144-7337

F.B. Cortés-Correa, is a BSc. in Chemical Engineer in 2004 from the Universidad Nacional de Colombia, Medellín, Colombia. Later, he graduated with an MSc. in Chemical Engineering and a PhD. in 2006 and 2009, respectively. Currently, he is an associate professor at the Department of Chemical and Petroleum Engineering in the Universidad Nacional de Colombia, Medellín, Colombia, and has been since 2011. He is the author of more than 40 published articles
ORCID: 0000-0003-1207-3859



UNIVERSIDAD NACIONAL DE COLOMBIA

SEDE MEDELLÍN

FACULTAD DE MINAS

Área Curricular de Ingeniería
Química e Ingeniería de Petróleos

Oferta de Posgrados

Maestría en Ingeniería - Ingeniería Química
Maestría en Ingeniería - Ingeniería de Petróleos
Doctorado en Ingeniería - Sistemas Energéticos

Mayor información:

E-mail: qcaypet_med@unal.edu.co
Teléfono: (57-4) 425 5317